

## MULTIPLLET EFFECTS IN NEAR EDGE XAS FOR GROUND STATE STUDIES

G. VAN DER LAAN, B.T. THOLE, J. ZAAENEN, G.A. SAWATZKY,  
J.C. FUGGLE\*, R.C. KARNATAK\*\* and J.M. ESTEVA\*\*

*Physical Chemistry Department of the Materials Science Center,  
Nijenborgh 16, NL-9747 AG Groningen, The Netherlands*

*\*Research Institute for Materials, University of Nijmegen,  
Toernooiveld 10, NL-6525 ED Nijmegen, The Netherlands*

*\*\*Laboratoire pour l'Utilisation du Rayonnement  
Electromagnétique, Bâtiment 209 D, Université Paris-Sud,  
F-91405 Orsay Cedex, France*

**ABSTRACT:** Manifold aspects of high resolution near edge absorption spectroscopy in the soft X-ray range can reveal interesting information on the nature of the ground state in various materials. One method uses the near edge multiplet structure of the final states, in which the optical selection rules limit the terms that can be reached from a given ground state. Thus the observed multiplet can be used to diagnose the ground state. This will be illustrated for Ce impurities and for Ni compounds

## 1-INTRODUCTION

The near edge structures in X-ray absorption spectroscopy (XAS) have regained much interest with the progress of synchrotron radiation sources, high resolution monochromators, efficient detection systems and ultra high vacuum technique. Simultaneously powerful computers have become available to perform calculations on radiation transition matrix elements in atomic configurations with several open shells /1/. These calculations can be used to determine the local ground state configuration of the X-ray excited atom in a solid. This has recently been demonstrated for all the rare earth metals /2/ and for Mn impurities /3/. Here, however, we will give examples of materials in which the ground state is a mixture of several configurations.

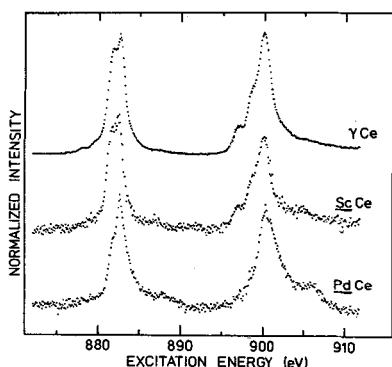
## 2-EXPERIMENTAL

X-ray absorption data were taken with the synchrotron radiation emitted by ACO (Orsay) using a double crystal monochromator equipped with beryl crystals (resolution 0.4 eV between 800 and 1000 eV). All spectra were recorded by electron yield detection. Ce compounds were mechanically scraped directly before measurements in a vacuum of better than  $5 \times 10^{-10}$  t. Ni compounds were sublimed in situ.

## 3-CERIUM ALLOYS

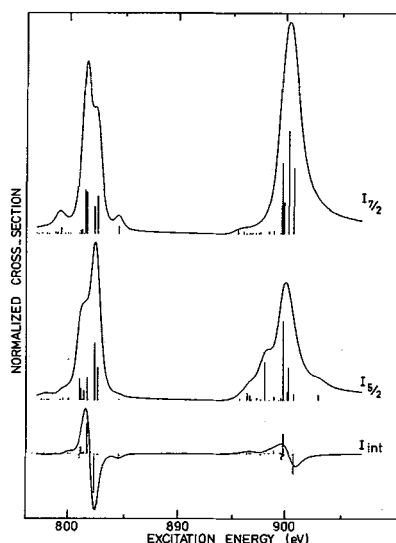
In the initial state the Ce  $4f^1$  state is split by spin-orbit coupling ( $\xi=107$  meV). The  $M_{4,5}$  absorption spectrum in  $\gamma$ Ce in Fig.1 displays the accessible multiplet structure for the transition  $3d^{10}4f^1(j=5/2) \rightarrow 3d^9 4f^2$ . Whilst in many Ce compounds and alloys the  $4f^1$  level is so weakly hybridized that only the lowest  $j=5/2$  level is occupied, in some Ce systems the hybridization with the valence band is so large that it mixes also the higher  $j=7/2$  level into the ground state. Whereas the  $M_{4,5}$  absorption spectrum for ScCe 2.3% is the same as for  $\gamma$ Ce, it is quite different, for PdCe 2.3%, indicating a large hybridization. In order to verify this, we have calculated the transition probability for the  $j=5/2$  and  $7/2$  initial state configurations, together with the interference term (Fig.2). The initial and final state wave functions, energies and optical matrix elements were calculated with an atomic Hartree-Fock program using empirically scaled values for the Slater integrals.

Comparison of the calculated spectra with the experimental data shows that  $\gamma\text{Ce}$  and  $\text{ScCe}$  2.3% have a  $j=5/2$  ground state, whereas in  $\text{PdCe}$  2.3% the ground state must have a  $4f(7/2)$  weight between 20 and 40 %. The increased intensity of the  $\sim 5$  eV satellite in the observed spectrum (Fig.1) is due to the  $4f^0$  contribution in the ground state as a consequence of the large hybridization /4/. The values obtained for the  $4f^0$ ,  $4f^1(5/2)$  and  $4f^1(7/2)$  weight are in agreement with those expected from the hybridization using the Gunnarsson-Schönhammer model /5,6/.



↑ Fig.1: The absorption spectra of  $\gamma\text{Ce}$ ,  $\text{ScCe}$  2.3% and  $\text{PdCe}$  2.3%.

→ Fig.2: The calculated  $\text{Ce } M_{4,5}$  absorption spectra for initial states  $j=7/2$  and  $5/2$  together with the interference term  $I_{\text{int}}$ .



#### 4-NICKEL COMPOUNDS

The beautiful variation in the spectral shape of the  $\text{Ni } L_{2,3}$  absorption edges for the  $\text{Ni}$  dihalides and  $\text{Ni}$  oxide is shown in Fig. 3. The  $L_3$  white line is roughly separated into two peaks (a and b). The separation decreases strongly in more covalent compounds. In the  $L_2$  region a similar behaviour is observed (e and f). Satellite structure (c) with a different shape for each compound is clearly observed at 3 to 7 eV above the  $L_3$  edge. Also at higher energy the  $4s$  continuum edge is visible (d).

A multiplet calculation for the dipole transitions  $\text{Ni } 3d^8 \rightarrow 2p^5 3d^9$  is shown in Fig.4, taking into account the octahedral crystal field and using Hartree-Fock values for the Coulomb and exchange integrals. As seen, this calculation agrees quite well for  $\text{NiF}_2$ , which is the most ionic compound. The differences in the spectra of the other compounds indicate that their ground state is not  $3d^8$ , but a mixture of several configurations /7/.

We therefore performed model calculations which take into account the configuration interaction in the initial as well as in the final state. In the initial state we have the configurations  $3d^8, 3d^9 k$  and  $3d^{10} k k'$  ( $k$  denotes a hole in the ligand band), schematically displayed in Fig.5. The energy separation of these states is equal to the charge transfer energy  $\Delta$ , which value strongly varies along the nephelauxetic series. For the  $3d^{10} k k'$  also the effective d-d Coulomb interaction  $U$  has to be included. The states with a ligand hole are broadened into bands. In the final state the separation of the centroids of the multiplet split  $2p^5 3d^9$  states and the  $2p^5 3d^{10} k$  band is different from the  $3d^9 k$  to  $3d^{10} k k'$  initial state separation, due to the corehole potential  $Q$ . For each irreducible representation in the symmetry group of the crystal field we can independently calculate the configuration interaction. This has been done with a cluster model as well as with the Gunnarsson-Schönhammer impurity model /5/. An example of the results is given for

NiI<sub>2</sub> in Fig.6. The satellite structure, which is due to the covalent mixing, is nicely reproduced in both models. The same type of calculation for the satellite structure can be used in XPS /8/ and UPS /9/ even though the spectral shapes in these methods are strongly different compared to XAS, due to the very different final states. The appearance of the satellite structure, with an energy separation from the main line equal, in first approximation, to  $\Delta + U - Q$  is a clear proof for important correlation effects in the Ni band /7,9/.

As seen in Fig.6, the clustermodel greatly overestimates the peak splitting in the white line, whereas the impurity model gives good agreement for all measured Ni compounds. The reason for this is that in the impurity model the atomic exchange integral  $G^1(2p,3d)$ , which dominates the multiplet splitting, is reduced by the hybridization with the valence band. In the cluster model this effect is underestimated.

The multiplet splitting in the main line can be used to obtain the relative populations and the energy separations of the initial state configurations. Further details can be found in Ref. /7/ and /9/. Note that here we only have studied compounds with octahedral symmetry in order to facilitate a direct comparison.

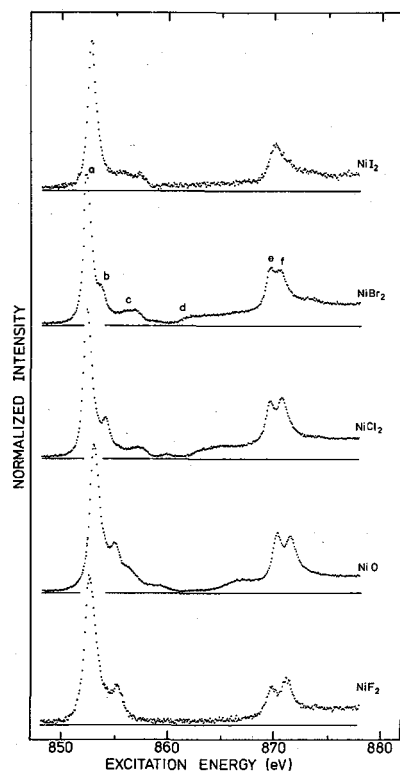


Fig.3:  $L_{23}$  absorption spectra of Ni compounds.

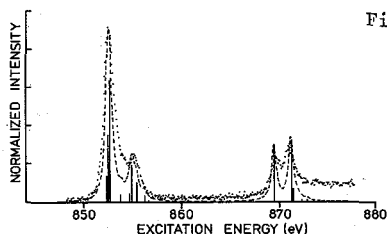


Fig.4

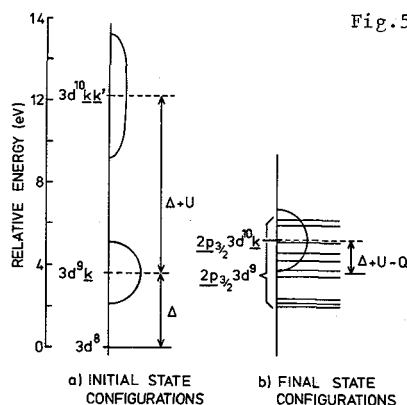
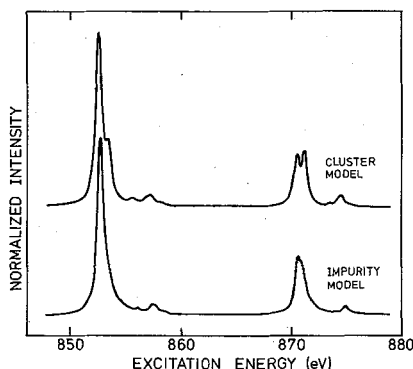


Fig.5

Fig.4: Calculated multiplet structure for a dipole transition  $Ni\ 3d^8 \rightarrow 2p^5 3d^9$  ( $G_1 = 5.79$ ,  $F_2 = 7.72$ ,  $G_3 = 3.29$  and  $10Dq = 1.5$  eV); the dashed line is a convolution by a 0.6 FWHM Lorentzian. For comparison, the experimental  $L_{23}$  spectrum of  $NiF_2$  is shown (dots).

Fig.5: Schematic representation of the energy for the different configurations: a) initial state; b) final states in the  $L_3$  absorption for the case of  $NiCl_2$ . Configurations with a ligand hole ( $k$ ) have a bandwidth  $W$ . The  $2p_{3/2} 3d^9$  configuration is multiplet-split. Not drawn is the mixing between the configurations.

Fig. 6: Clustermodel and impurity model compared for the case of  $\text{NiI}_2$  ( $\Delta = 1$  eV).



##### 5-CONCLUDING REMARKS

The use of X-ray absorption near edge structure to diagnose chemical environments as well as the site and symmetry characteristics of unoccupied electronic states, has a long history [11,12]. However it is only in the last few years that experimental and computational technology has sufficiently advanced to permit utilization of the multiplet structure that arises near the edges in narrow band materials. In this paper we have shown that although we have used excitation energies in the order of 1 KeV, and multiplet splittings on a scale of many volts, we have been able to probe ground state splittings of  $\sim 100$  meV and give details of the ground state configurations. In other work [13] we have been able to detect splittings which only become observable below ca 60 Kelvin (i.e.  $kT = 5$  meV).

By comparison with other techniques, such as those based on low energy optical or magnetic transitions XAS in the soft X-ray regime has rather special properties. These include moderate surface sensitivity and applicability to thin films, well defined site and symmetry selectivity, and well defined final states. These, and other features convince us that the aspects of XAS treated here have until now been underexploited.

##### REFERENCES:

- 1- R.D.Cowan, "The Theory of Atomic Structure and Spectra" (Univ. of California Press, Berkeley, 1981)
- 2- B.T.Thole, G. van der Laan, J.C.Fuggle, G.A.Sawatzky, R.C.Karnatak and J.M. Esteve, Phys. Rev. B32, 5107 (1985).
- 3- B.T.Thole, R.D.Cowan, G.A.Sawatzky, J.Fink and J.C.Fuggle, Phys. Rev. B31, 5107 (1985).
- 4- J.C.Fuggle, F.U.Hillebrecht, J.M.Esteve, R.C.Karnatak, O.Gunnarsson and K. Schönhammer, Phys. Rev. B27, 4637 (1983).
- 5- O.Gunnarsson and K. Schönhammer, Phys. Rev. B28, 4315 (1983); J.Zaanen, G.A. Sawatzky and J.W.Allen, Phys. Rev. Lett. 55, 418 (1985).
- 6- G.van der Laan, J. Zaanen, G.A.Sawatzky, J.C.Fuggle, R.C.Karnatak, J.M.Esteve, and B.Lengeler, J.Phys.C: Solid State Phys.19, 817 (1986).
- 7- G.van der Laan, J.Zaanen, G.A.Sawatzky, R.C.Karnatak and J.M.Esteve, Solid State Commun. 56, 673 (1985).
- 8- G.van der Laan, C.Westra, C.Haas, and G.A.Sawatzky, Phys. Rev. B23, 4369 (1981).
- 9- G.van der Laan, Solid State Commun. 42, 165 (1982).
- 10- G.van der Laan, J.Zaanen, G.A.Sawatzky, R.C.Karnatak, and J.M.Esteve, Phys. Rev. B33, 4253 (1986).
- 11- L.G.Parratt, Rev. Mod. Phys. 31, 616 (1959) and ref. therein.
- 12- D.J.Fabian, L.M.Watson and C.A.W.Marshall, Rep. Prog. Mod. Phys. 34, 601 (1971) and ref. therein.
- 13- G.van der Laan, B.T.Thole, G.A.Sawatzky, J.B.Goedkoop, J.C.Fuggle, J.M.Esteve, R.C.Karnatak, J.P.Remeika and H.A.Dabkowska, Phys. Rev. B, accepted for publication.